Organic Electronics 58 (2018) 53–62

Contents lists available at ScienceDirect

Organic Electronics

journal homepage: www.elsevier.com/locate/orgel

Review

High efficiency small molecule-based donor materials for organic solar cells

Rashid Ilmi, Ashanul Haque, M.S. Khan*

Department of Chemistry, Sultan Qaboos University, Al-Khod, Oman

ARTICLE INFO

Keywords:
Small donor molecules
Molecular design
Organic solar cells

ABSTRACT

Organic photovoltaic (OPV) materials, especially small molecule donor materials (SMDMs) have enormous potential to revolutionize the solar energy sector. However, to be a viable alternative to the polymer donor counterparts, SMDMs must have high power conversion efficiency (PCE). A large number of different SMDMs have been reported, which have crossed the 10% threshold of the PCE for commercialization. In this review, we present the SMDMs that have been developed in recent years capable of generating moderate to high-efficiency photovoltaic devices. The steady rise in the variety of materials and PCE values in recent years, point to a bright future for SMDMs as solar energy materials.

1. Introduction

Solar energy is one of the most powerful alternatives to non-renewable fossil fuels. Unfortunately, we are unable to harness the full potential of the solar energy, partially due to engineering challenges and largely due to the lack of efficient photovoltaic (PV) cells, which convert sun light to electrical energy. Based on the solid-state electronic material system used, a PV cell can be divided into crystalline elemental (silicon), organic, thin-film (CIGS, CdTe, amorphous Si) or hybrid [1]. At present, the PV market is dominated (> 90%) by the crystalline, polycrystalline and amorphous inorganic materials based solar cells [2]. Despite the fact that these solar cells (SCs) have excellent light to electricity conversion ability, their high manufacturing cost, slow manufacturing, sensitivity to impurities, low-flexibility, etc. pose significant challenges to the industrial and individual consumers [3]. To overcome these challenges, organic photovoltaic (OPV) cells emerged as a promising alternative. Organic semiconductors are conjugated materials that conduct electricity when they reach sufficient number of alternating single and double bonds and have conductivity between a metal and an insulator (10^{-9} to $10^{3}\ \Omega^{-1}\ cm^{-1}$) [4]. Organic materials have several advantages over inorganic semiconductors like high absorption coefficient and broad absorption range, which can be tuned by chemical functionalization. The easy functionalization of organic semiconductors is a prime advantage that surpasses all advantages of inorganic semiconducting materials. The last decade witnessed a tremendous rise in the development of the OPVs with a high power conversion efficiency (PCE) [5] using organic donor material. Although the value is lower than their inorganic counterparts, it's sufficient for use, which is set at 10% [6].

Based on the type of molecular system used, OPV is divided into two classes: polymer-donor solar cells (PDSCs) and small molecule-donor solar cells (SMDSCs). Interestingly, the efficiency of SMDSCs have increased considerably from 0.001% in 1975 [7], through 1% in 1986 [8] to > 11.3% in 2017 [9,10], which is very close to the highest value obtained by any OPV cells (PDSCs ~ 13%) [11]. This incredible rise in performance has been possible due to several advantages offered by the SMDMs, e.g., synthetic ease, synthetic reproducibility with high purity, discrete molecular weight, well defined molecular structure, low weight and cost, mechanical flexibility, suitability for large area applications and high charge carrier mobility, etc. [12–14]. Considering the importance of this rapidly developing field, we present herein the progress made in recent years in the development of SMDMs for OPV. Fig. 1 depicts result generated by Web of Science when searched for the term "Organic Small Molecule Solar Cells" during the time interval of 2010–2017. A total of 553 articles have been published since the beginning of 21st century, which is still on the rise. Furthermore, citation related to this topic has also grown tremendously. Both PDSCs and SMDSCs have been reported in the literature. In the succeeding sections, attempts have been made to discuss progress made in the development of SMDSCs for OPV.

2. Performance parameters of solar cells (SCs)

There are many excellent articles and books which chronicles the structure and mechanism of PV devices [15–20]. We herein discuss briefly the performance parameters that are required for characterizing SCs. Generally, the OSCs are characterized under a 1000 W/m^2 light with the spectrum matching that of the sun on the earth's surface at an

* Corresponding author.
E-mail addresses: msk@squ.edu.om, msk.squ.edu@gmail.com (M.S. Khan).

https://doi.org/10.1016/j.orgel.2018.03.048
Received 29 November 2017; Received in revised form 29 January 2018; Accepted 27 March 2018
Available online 29 March 2018

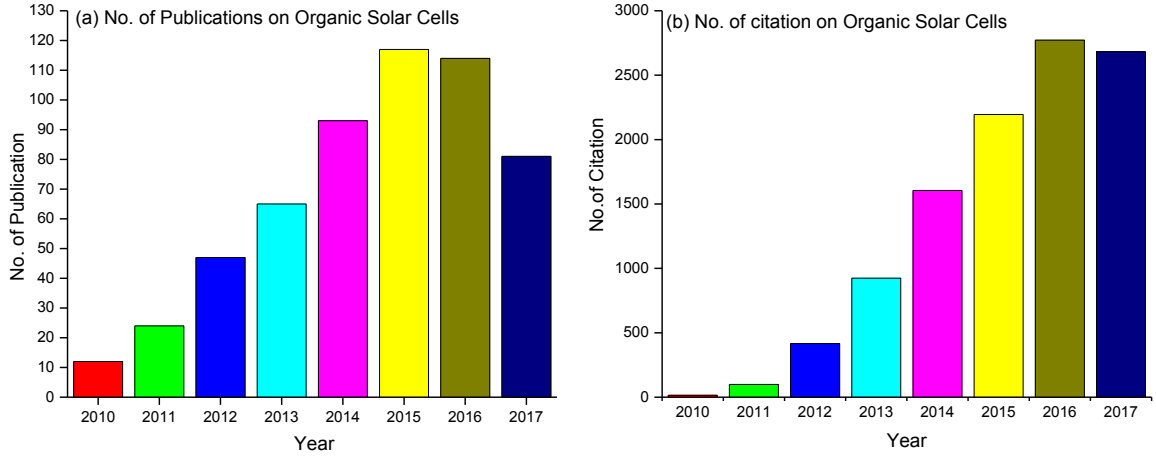

Fig. 1. Histogram showing the number of scientific publications contributing to the subject "Organic SC(s)" by the year. The period was **2010–2017** and the keyword was "Organic Small Molecule Solar Cells". Search done through ISI, Web of Science.

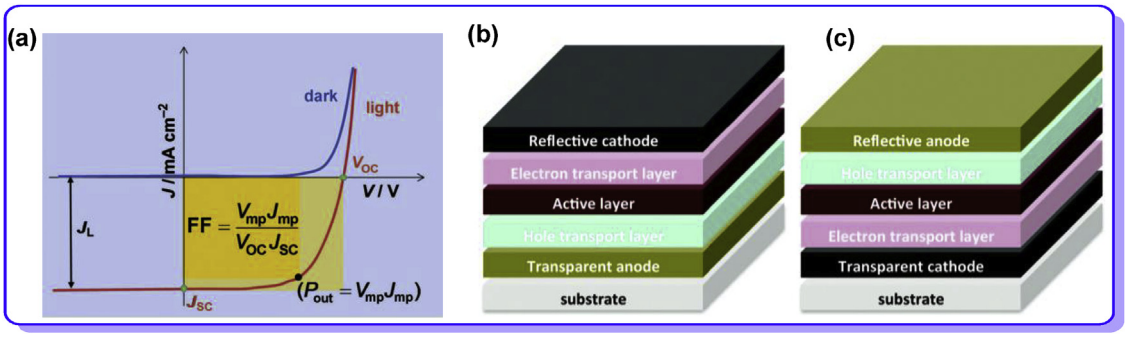

Fig. 2. (a) A typical current-voltage *J-V* characteristics of solar cells. (b) standard architecture of bulk-heterojunction (BHJ) and (c) inverted structure. Reproduced with the permission of Ref. [17] and [30].

incident angle of 48.2° (called the AM 1.5 spectrum) [21]. A typical current–voltage (I-V) curve of a SC in the dark and under illumination are shown in Fig. 2a along with the structures of standard PV cells (Fig. 2b and c). In the dark, there is almost no current until the forward bias for voltages is larger than the open circuit voltage (V_{OC}). Under illumination, the SCs start generating power which is recorded with a source meter. For characterization of any SC, the key parameter is the PCE, which is the ratio of the maximum electrical power (P_m) generated by the device to the total incident optical power (P_{in}) (equation (1)). P_{in} is given by the spectral intensity matching the sun's intensity on the Earth at an angle of 48.2° (equivalent to AM 1.5 spectrum) [22].

$$\eta_e = \frac{P_m}{P_{in}} \times 100 = \frac{V_{OC} \times I_{SC} \times FF}{P_{in}} \times 100 \quad (1)$$

The term V_{oc} in Eq. (1) is defined as the potential at which current is zero and depends on HOMO and LUMO energy level difference of the donor (D) and acceptor (A). Therefore, the V_{oc} of the SC can be increased either by reducing the HOMO level of the donor or increasing the LUMO level of the acceptor material. The second term in Eq. (1) J_{sc} is a maximum generated photocurrent density. As the band-gap of the material decreases, the value of J_{sc} increases and can be affected by the electron and hole transport efficiency of the active material [23]. The third term is the fill factor (FF) and is defined as the ratio of observed maximum power output to the theoretical power output. Maximum power output is given by P_m (= I_m x V_m), and the theoretical output is the product of J_{sc} and V_{oc}, therefore, the FF can be defined by Eq. (2).

$$FF = \frac{J_{MP} \times V_{MP}}{J_{SC} \times V_{OC}} \quad (2)$$

The FF suggests how swiftly the charges can be removed from the cells and in an ideal case the value is 1.0. There are a number of factors that can affect the FF of SCs and they often interact in intricate ways. The series resistance (R_s), parallel resistance (R_{sh}) are two other important factors that affect the FF and performance of SCs. The physical phenomena governing J_{sc} [24,25] and V_{oc} [26–28] have been well documented. However, factors affecting the FF is still not so clearly understood [29].

3. SMDMs–based photovoltaics

Several reviews have chronicled the progress made on SMDMs–based PV cells [30,31]. Herein we have reviewed only very recent articles with moderate to high PCE.

3.1. Oligothiophene-based SMDMs

During the literature survey, we noted that most of SMDMs are based on electron-rich thiophene units, supporting the importance of this heterocyclic core in materials science. Sulphur containing heterocycles such as simple thiophene, fused and non-fused oligothiophenes, and their derivatives are commonly employed as electron-donor units. The electronic properties and bulk-heterojunction (BHJ) SC parameters of some recently reported oligothiophene based SMDMs are summarized in Table 1. The results indicate that structurally simple SMDM molecules are potential candidates as donor for achieving highly efficient OSCs. Liu et al. [32] reported an oligo-thiophene (n = 7) based small donor **1** (Chart 1) composed of 3-octylthiophene as the central donor decorated with 3-ethylrhodanine at the periphery. The electron withdrawing nature of 3-ethylrhodanine created a strong donor-acceptor (D-A) interaction within the oligomer, leading to absorption in

Table 1
Summary of frontier energy levels, device structure and performance parameters of oligothiophene-based SMDMs.

Entry	HOMO/LUMO (eV)	Device architecture	V_{OC} (V)	J_{sc} (mA/cm^2)	FF (%)	PCE (%)	Ref.
1	−5.00/−3.28	ITO/PEDOT:PSS/**1**:$PC_{61}BM$/LiF/Al	0.92	13.98	47.4	6.10	[32]
2	−5.18/–2.68	ITO/PEDOT:PSS/**2**:$PC_{71}BM$/LiF/Al	0.86	10.26	66.8	5.89	[33]
3	−5.28/–2.80	ITO/PEDOT:PSS/**3**:$PC_{71}BM$/LiF/Al	0.93	11.03	69.6	7.14	[33]
4a	−5.52/–3.23	ITO/PEDOT:PSS/**4a**/Ca/Al	0.62	1.37	48.2	0.41	[34]
4b	−5.24/–3.61	ITO/PEDOT:PSS/**4b**/Ca/Al	0.82	5.32	49.2	2.16	[34]
4c	−5.32/–3.63	ITO/PEDOT:PSS/**4c**/Ca/Al	0.83	4.00	50.9	1.69	[34]
4d	−5.22/–3.69	ITO/PEDOT:PSS/**4d**/Ca/Al	0.78	6.59	46.9	2.40	[34]
4e	−5.16/–3.57	ITO/PEDOT:PSS/**4e**/Ca/Al	0.76	3.63	57.0	1.57	[34]
5	−5.12/−3.19	Glass/ITO/PEDOT:PSS/**5**/PrC60MA/Al	0.96	14.59	66.0	9.23	[35]
6	−5.10/−3.45	Glass/ITO/MoO_3/**6**:$PC_{71}BM$/LiF/Al	0.79	12.98	49.0	5.04	[36]
7a	−5.38/−3.32	Glass/ITO/PEDOT:PSS/**7a**:$PC_{61}BM$/Al	0.97	7.93	64.1	4.87	[39]
7b	−5.25/−3.25	Glass/ITO/PEDOT:PSS/**7b**:$PC_{61}BM$/Al	0.90	1.36	32.7	0.39	[39]
7c	−5.31/−3.43	Glass/ITO/PEDOT:PSS/**7c**:$PC_{61}BM$/Al	1.00	1.50	27.5	0.41	[39]
8a	−5.38/−3.71	ITO/PEDOT:PSS/**8a**:$PC_{71}BM$/PDINO/Al	0.79	12.88	65.8	6.68	[40]
8b	−5.25/−3.61	ITO/PEDOT:PSS/**8b**:$PC_{71}BM$/PDINO/Al	0.88	10.08	48.9	4.33	[40]
8c	−5.15/−3.68	ITO/PEDOT:PSS/**8c**:$PC_{71}BM$/PDINO/Al	0.87	7.21	52.5	3.30	[40]

PEDOT:PSS = poly(3,4-ethylenedioxythiophene):polystyrene sulfonate, PDINO = perylenediimide *N*-oxide.

visible region with low band gap (E_g°) of 1.72 eV. Oligomer **1** produced high quality thin film through solution processing technique and showed broad absorption in visible region (450–750 nm) with λ_{max} = 618 nm with red-shift of ~110 nm compared to parent molecule **1** in chloroform ($CHCl_3$). Using **1** as donor and $PC_{61}BM$ as acceptor (Chart 1), they achieved a high PCE (6.10%) with V_{oc} of 0.92 V and J_{sc} of 13.98 mA/cm^2. An increase in the number of thiophene units in the central core (n = 8) with elongation of alkyl chain at the termini (**2**, Chart 1) did not affect the PV performance too much. However, a significant improvement in the PCE and other parameters were noted upon the fluorination of central thiophenes (**3**, Chart 1) [33]. Both SMDs displayed broad absorption with good thermal stability; however, the fluorinated analogue had comparatively deeper HOMO energy level. The fluorination of the central unit induces better planarity in SMD **3** (dihedral angle of 0.52° between two thiophenes) than non-fluorinated SMD **2** leading to enhanced molecular packing and carrier mobility. Under optimized conditions, an inverted PV cell based on **3** gave a PCE ~7.14%. Liang et al. [34] designed and synthesized D2-A-D1-A-D2 type of SMDs (**4a-e,** Chart 1) and systematically studied the effect of the number of thiophene units on the PCE of the fabricated device (Table 1). They concluded that the SMDs with odd number of thiophene unit(s) have higher PCE compared to the ones having even number of thiophene units. Zhang et al. [35] designed and synthesized a new SMD **5** (Chart 1) composed of planar electron-withdrawing 1,3-bis(4-(2-ethylhexyl)-thiophen-2-yl)-5,7-bis(2-ethylhexyl) benzo[1,2-c:4,5-c′]-dithiophene-4,8-dione (BDD) unit as the central core. After thermal annealing (TA) and solvent vapor annealing (SVA), a PCE of 9.35% was achieved with high values of V_{oc}, J_{sc} and FF (Table 1). The high value of V_{oc} was attributed to the low HOMO energy level while high J_{sc} and FF values were attributed to the enhanced absorption of blend films, fine-tuned morphology and good charge mobilities. These results suggest that an electron-withdrawing central unit with a large planar structure and A–D–A configuration is an efficient way to achieve high-performance PV cells. Hong et al. [36] designed and synthesized a new SMD **6** (Chart 1), having dithieno[3,2- b:2′,3′- d]phosphole oxide (DTP) as the central core and 3-ethylrhodanine as termini separated by alkyl terthiophene. Since the DTP molecule forms an unusual hyperconjugated ring with rigid pyramidal geometry, which lowers the energy level of LUMO and making them strong electron acceptor [37,38]. The absorption spectrum of SMD **6** in solution and in thin film showed a broad absorption range (300–750 nm) with maxima at 516 nm, which was 78 nm red-shifted in thin film due to intermolecular π–π stacking (Fig. 3). SMD **6** exhibited an emission peak at 724 nm which was significantly quenched (97%) in the **6**:$PC_{71}BM$ blend film (due to the polarizable nature of the DTP moiety and superior miscibility between **6** and $PC_{71}BM$). The BHJ device based on **6** exhibited a PCE value of 5.04% with a J_{sc} of 12.98 mA/cm^2, a V_{oc} of 0.79 V. These promising PCE values were achieved without any pre- or post-treatments and suggesteing that DTP-based small molecule can be a promising candidate for PV application.

Chen and co-workers [39] assessed BHJ-SCs based on *cis*-stilbene with or without a spiro linker, terthiophene arms and acceptor end groups **7(a–c)** (Chart 1). They reported that BHJ composed of spiro-containing molecule **7a** showed better light-harvesting ability than **7b**. The device based on the **7a** and $PC_{71}BM$ with 1,8-diiodooctane (DIO) additive exhibited uniform and optimal domains with better percolation length in the film leading to PCE of 4.87% and a high FF of 64.1%. Along similar line Wang et al. [40] designed and synthesized three A-π-

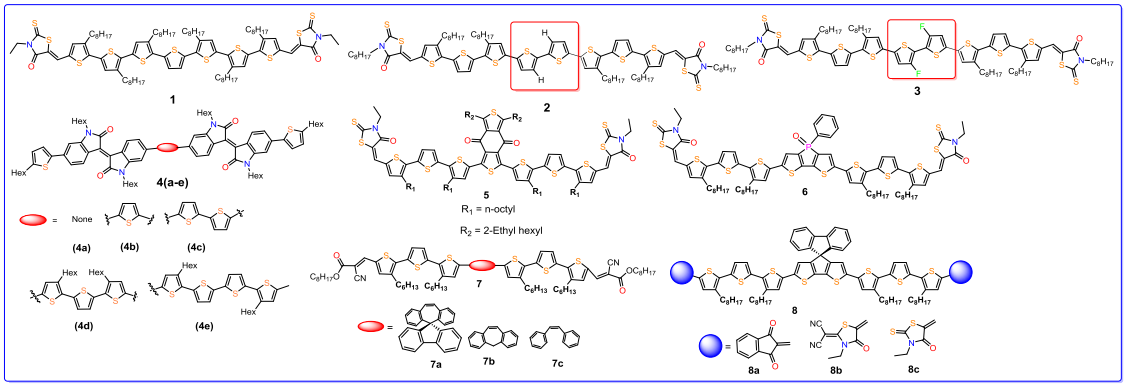

Chart 1. Oligothiophene-based SMDMs.

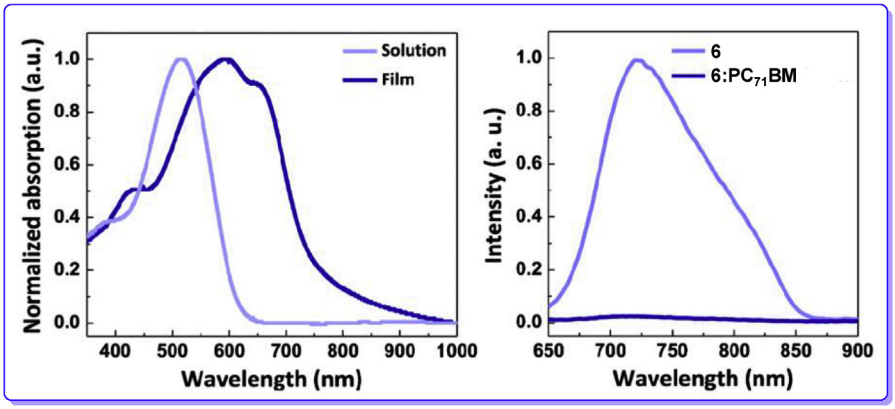

Fig. 3. (a) Normalized UV–vis–NIR absorption spectra of **6** in $CHCl_3$ solution or as a thin film; (b) PL spectra of pure **6** and **6**:$PC_{71}BM$ blend films. Reproduced with the permission of Ref. [36].

D-π-A SMD **8** with spiro[cyclopenta[1,2-b:5,4-b′]dithiophene-4,9′-fluorene] (STF) as the central donor core. The SMDs **8(a–c)** (Chart 1), showed wide absorption bands (300–850 nm) with high molar absorption coefficients (4.82×10^4 to $7.56 \times 10^4\ M^{-1}\ cm^{-1}$) and relatively low HOMO levels (−5.15 to −5.38 eV). The optimized OSCs based on these molecules deliver PCEs of 6.68%, 3.30%, and 4.33% for **8a**, **8b**, and **8c**, respectively. The higher PCE of **8a**-based OSCs was attributed to its better absorption ability, higher and balanced charge mobilities, and superior active layer morphology. In fact, this was the first example of developing the A-π-D-π-A type small molecules with a spiro-central donor core for high-performance OSC applications.

3.2. Oligothiophene-benzodithiophene (BDT) hybrids as SMDMs

In addition to thiophene and oligothiophenes based SMDMs, several benzodithiophene (BDT) based hybrid materials have also been investigated recently (Chart 2). Table 2 shows the performance of OPV based on BDT hybrids. When fluorinated 2,2'-bithiophene unit was replaced by BDT and 3-ethylrhodanine by cyano functionalities, the resulting SMD **9** (Chart 2) generated a PCE of 4.56% in combination of $PC_{61}BM$ as acceptor [41]. Interestingly, when 3-ethylrhodanine was installed back on SMD **10** (Chart 2), it led to a sharp increase in PCE (6.38%) and significant rise in current density (J_{sc} = 10.78 mA cm^{-2}). The enhanced performance was attributed to the better light absorption of **10** compared to **9** [41]. Furthermore, when the acceptor was changed to $PC_{71}BM$, device based on **9** gave a significantly low efficiency as well as current density (PCE = 2.09%, J_{sc} = 3.74 mA/cm^2) while device based on **10** yielded an improved PCE (6.92%) and J_{sc} (11.40 mA/cm^2). All these PV parameters reached maximum values (PCE = 7.38%, V_{oc} = 0.93 V, J_{sc} = 12.21 mA/cm^2) by the addition of trimethylsiloxyl terminated polydimethylsiloxane (PDMs) during the film-forming process. These results clearly show that not only the acceptor but other additives also impact the performance of the device. Studies showed that the replacement of alkoxy group over BDT by alkyl [42] and thioether [43] also improves the device performance. For example, using oligomer **11** (Chart 2), PCE of about 8.26% was reported, while **12** (Chart 2) based device gave a maximum PCE of 9.95% [42,43]. It is worthwhile to note that the enhanced performance could not be attributed to the structure modification only but also to the morphology, absorption profile and structure of the active layer. The introduction of an extra alkylthio-thiophene as side chains on the BDT unit (**13,** Chart 2) resulting a PCE of 9.20% without any processing [44]. Interestingly, **13**:$PC_{71}BM$ based device with active area of 14.4 cm^2 generated PCE of 6.68%. A slight increase in performance (annealing dependent) was reported for devices based on donor **14** (9.6%) [45] and **15** (9.3%) [46] (Chart 3) bearing more branched side chains. Not only this, **14**-based device also afforded high fill factor (FF ~ 70%) and PCE (~8%) at the active layer thicknesses up to 400 nm.

In order to commercialize OSCs, the successful demonstration of PV devices via printing method is essential to apply them into the roll-to-roll process. To verify the effect of the roll-to-roll compatible approach, Heo et al. [47] used small molecule **15** and fabricated three types of devices: (a) as cast films without any treatment, (b) blend films following the SVA treatment and (c) blend films processed with a diphenyl ether (DPE) additive slot-die printed devices with a normal structure of ITO/PEDOT:PSS/**15**:$PC_{71}BM$/Ca/Al. The device (a) without any treatment showed PCE of 3.81%. The device (b) showed enhanced PCE of 7.46%, as reported earlier [46]. Interestingly, DPE processed devices also exhibited high PCE (6.56%), due to a significant increase in FF and J_{sc}, even though there were slight drops in V_{oc}. Furthermore, authors also achieved a PCE of 4.80% using large-area (10 cm^2) PV modules (Fig. 4). These results signify the potential of SMDMs in the large-scale production of OSCs via roll-to-roll compatible printing methods without using halogenated solvent.

Badgujar et al. [48] synthesized (**16** and **17,** Chart 2) and conducted a comparative study of the device performance by increasing the number of BDT units in the SMD core. They found that the increase in the number of BDT units in **17** gives rise to strong intermolecular interaction, which promoted the desired interconnected structure and therefore, enhanced exciton diffusion and free-charge-carrier transport as compared to **16**. The device based on **17** showed PCE of 8.56% with a high FF (73%) under AM 1.5 G irradiation (100 mW /cm^2). Since this PCE is achieved without any additive, the result is unambiguously important for high reproducibility and fabrication of large-area modules. The performance of the device based on **17** with an area of 777.5 cm^2 showed PCE of 7.45% compared to 4.5% as shown by **16** (Fig. 5a). In similar aspect, Guo et al. [49] designed and synthesized two unsymmetrical BDT core monomer **18** and dimer **19** (Chart 2). The dimer was connected by octamethylene spacer. The device based on monomer **18** showed a higher PCE (8.18%) compared to the dimer **19** (7.07%). The lower PCE of the dimer was blamed to lower J_{sc} (10.88 mA /cm^2), which in turn related to the poor absorption profile (Fig. 5b), low internal quantum efficiency and photo-induced charge transfer in the dimer.

In another very interesting study Deng et al. [10] combined a traditional molecular design with fluorination. They designed and synthesized three SMDs (**20a-c**, Chart 2) with increasing number of fluorine atoms, **20a**, **20b** and **20c**. The designed molecules showed optimal morphology which is important for charge transfer, charge collection and recombination suppression leading to reduced loss of V_{oc}, J_{sc} and FF simultaneously. As a consequence, fluorinated molecules exhibited excellent inverted device performance, and an average PCE of 11.08% and FF 76.0% was achieved with **20c** having two fluorine

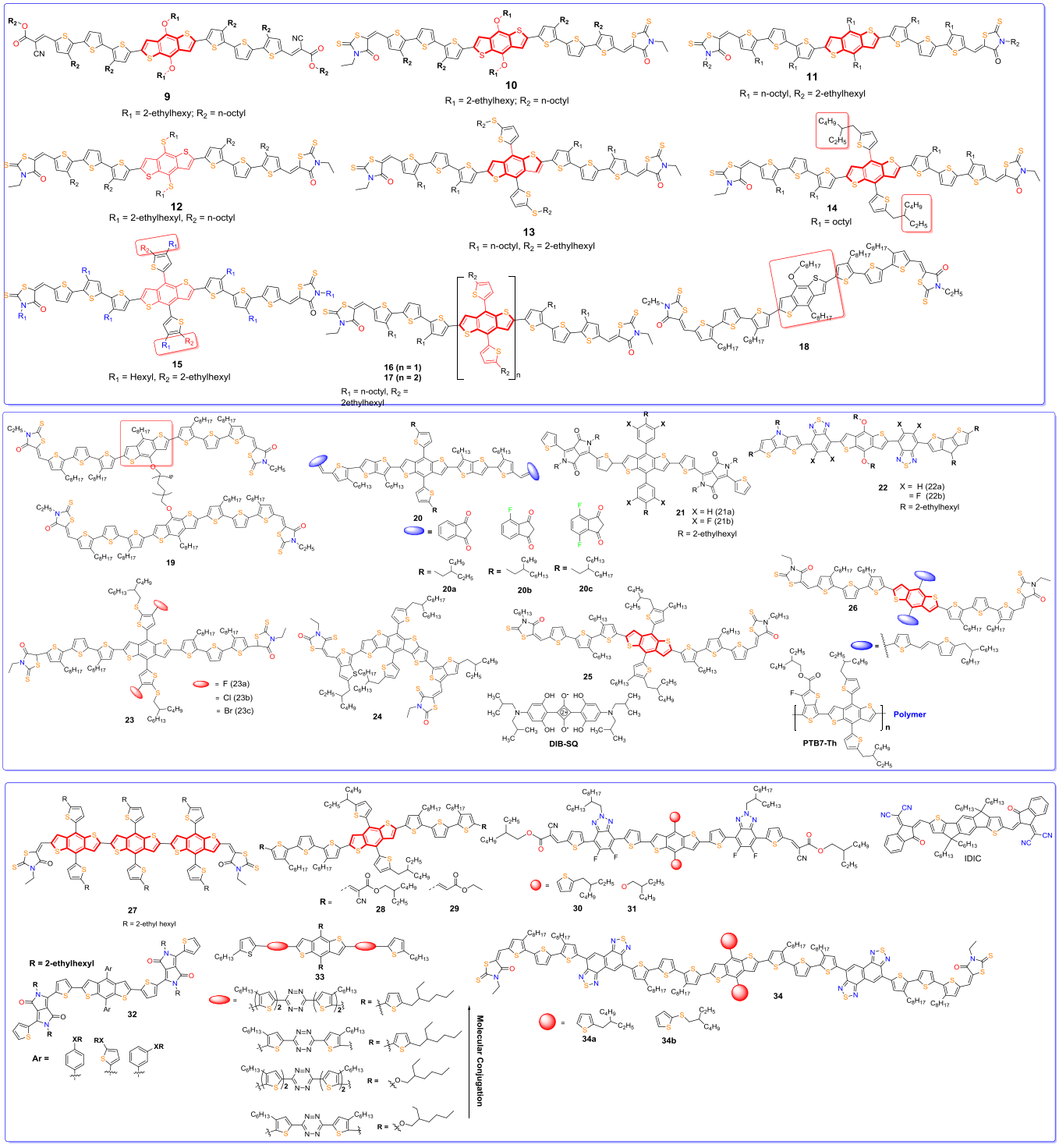

Chart 2. Chemical structures of benzodithiophene (BDT) hybrids used as SMDMs.

atoms. With very similar strategy, Eastham et al. [50] designed two new small molecule based on diketopyrrolopyrrole–benzodithiophene–diketopyrrolopyrrole (BDT-DPP$_2$) skeleton with and without fluorine on the aromatic side chains **21a** and **21b** (Chart 2). The ternary SC with varying ratios of two SMDs and PC$_{61}$BM resulted in tunable V_{oc} (0.833–0.944 V) due to a fluorination-induced shift in energy levels and the electronic "alloy" formed from the miscibility of the two SMDs. A 15% increase in PCE is observed at the optimal ternary SMD ratio, with significantly increased J_{sc} (9.18 mA/cm^2), due to the increased optical absorption of the blend. Busireddy et al. [51] designed and studied the effect of fluorination on PV performances of two small D$_1$–A–D$_2$–A–D$_1$ type skeleton having 2,4-bis(2-ethylhexyl)-4*H*-dithieno[3,2-b:2′,3′-*d*] pyrrole (EHDTP, D$_1$) and 4,8-bis((2-ethylhexyl)oxy) benzo[1,2-b:4,5-b′] dithiophene (OBDT, D$_2$) as the terminal and central donor, and benzo [*c*][1,2,5] thiadiazole (**22a**) and 5,6-difluorobenzo[*c*][1,2,5]thiadiazole (**22b**) (Chart 2). The fabricated BHJ-SCs with two-step annealed (thermal followed by SVA) active layers of **22a** and **22b** showed overall PCE of 5.46% and 7.91%, respectively. The superior performance of the **22b** based device was attributed to the favorable morphology and nanoscale interpenetrating network in the **22b**:PC$_{71}$BM active layer. This

Table 2
Summary of frontier energy levels, device structure and performance parameters of oligothiophene-Benzodithiophene (BDT) hybrids.

Entry	HOMO/LUMO (eV)	Device architecture	V_{OC} (V)	J_{sc} (mA/cm^2)	FF (%)	PCE (%)	Ref.
9	−5.04/−3.24	Glass/ITO/PEDOT–PSS/**9**/LiF/Al	0.93	3.74	60.1	2.09	[41]
10	−5.02/−3.27	Glass/ITO/PEDOT–PSS/**10**/LiF/Al	0.93	12.21	65.0	7.38	[41]
11	−5.08/−3.27	ITO/(PEDOT-PSS)/**11**:$PC_{71}BM$/ZnO/Al	0.94	12.56	70.0	8.26	[42]
12	−5.07/−3.30	ITO/PEDOT:PSS/**12**:$PC_{71}BM$/ETL-1/Al	0.91	14.45	73.0	9.60	[43]
13	−5.18–3.25	ITO/PEDOT:PSS/**13**:$PC_{71}BM$/Ca/Al	0.97	13.45	70.5	9.20	[44]
16	−5.14/−3.37	ITO/PEDOT:PSS/**16**: $PC_{71}BM$/Ca/Al	0.89	13.02	62.0	7.18	[48]
17	−5.13/−3.37	ITO/PEDOT:PSS/**17**: $PC_{71}BM$/Ca/Al	0.89	13.17	73.0	8.56	[48]
18	−4.94/−3.30	ITO/PSS:PEDOT/**18**:$PC_{71}BM$/ETL-1/Al	0.87	12.54	74.0	8.18	[49]
19	−5.02/−3.30	ITO/PSS:PEDOT/**19**:$PC_{71}BM$/ETL-1/Al	0.86	10.62	72.0	7.07	[49]
20a	−4.91/−3.20	ITO/ZnO/**20a**/MoO_x/Ag	0.93	14.0	64.0	8.3	[10]
20b	−4.98/−3.28	ITO/ZnO/**20b**/MoO_x/Ag	0.94	15.3	72.0	10.4	[10]
20c	−5.05/−3.37	ITO/ZnO/**20c**/MoO_x/Ag	0.95	15.7	76.0	11.3	[10]
21a	−5.36/−3.66	ITO/PEDOT:PSS/**21a**: $PC_{71}BM$/LiF/Al	0.83	8.36	59.6	4.15	[50]
21b	−5.47/−3.75	ITO/PEDOT:PSS/**21b**: $PC_{71}BM$/LiF/Al	0.94	7.81	57.8	4.26	[50]
22a	−5.55/−3.65	ITO/PEDOT:PSS/**22a**: $PC_{71}BM$/PFN/Al	0.91	10.52	57.0	5.46	[51]
22b	−5.66/−3.69	ITO/PEDOT:PSS/**22b**: $PC_{71}BM$/PFN/Al	0.98	12.23	66.0	7.91	[51]
23a	−5.05/−2.88	ITO/PEDOT:PSS/**23a**: $PC_{71}BM$/Ca/Al	0.95	14.31	68.9	9.37	[52]
23b	−5.06/−2.88	ITO/PEDOT:PSS/**23b**: $PC_{71}BM$/Ca/Al	0.96	14.92	75.3	10.78	[52]
23c	−5.06/−2.89	ITO/PEDOT:PSS/**23c**: $PC_{71}BM$/Ca/Al	0.98	13.85	63.1	8.55	[52]
24	−5.06/−3.45	ITO/PEDOT:PSS/**24**:$PC_{71}BM$/Ca/Al	0.90	13.33	67.0	8.17	[53]
25	−5.38/−3.61	Ternary	0.90	15.44	73.8	10.3	[57]
25	−5.38/−3.61	Ternary	0.75	21.4	70.0	11.40	[58]
26	−5.29/−3.27	Ternary	0.77	14.52	70.3	7.77	[59]
27	−5.29/−3.34	ITO/MoO_3/**27**:IC-C6IDT-IC/Al	0.98	14.25	65.0	9.08	[60]
28	−5.24/−2.82	ITO/PEDOT:PSS/**28**:IDIC/PDINO/Al	0.90	15.18	73.55	10.11	[61]
29	−5.04/−2.70	ITO/PEDOT:PSS/**29**:IDIC/PDINO/Al	0.76	10.77	64.40	5.32	[61]
30	−5.31/−3.03	ITO/PEDOT:PSS/**30**:IDIC:PDINO/Al	0.977	15.21	65.46	9.73	[62]
31	−5.28/−3.01	ITO/PEDOT:PSS/**31**:IDIC:PDINO/Al	0.955	10.51	54.89	5.51	[62]

PEDOT:PSS = poly(3,4-ethylenedioxythiophene):polystyrene sulfonate, PDINO = perylenediimide N-oxide, PFN = poly(9,9-bis(3′-(N,N-dimethylamino)propyl) fluorene-2,7-diyl)-alt-(9,9-dioctylfluorene-2,7-diyl).

was induced by the fluorine atoms on the BT acceptor, which significantly enhanced the dissociation of excitons, charge transport and the charge collection efficiency, and suppressed bimolecular recombination in the BHJ. The observed higher PCE indicated **22b** is one of the best BT based donor materials for small molecular BHJ-SCs.

Ji et al. [52] investigated the effect of molecular structure i.e., halogenation on the properties and consequently on the PV performance. They reported three new SMDs (**23 a-c**, Chart 2) incorporating BDT central core having different halogen atoms (fluorine, chlorine and bromine) and 3-ethylrhodanine as the terminal groups. Due to the presence of fluorine atom in SMD, film composed of **23a**:$PC_{71}BM$ showed a high degree of crystallinity and poor phase of blend film. Replacing fluorine by chlorine (**23b**) and bromine (**23c**) led to decreased crystallinity; however, strong aggregations were effectively suppressed. The fabricated device with the Cl-bearing SM (**23b**) exhibited the best PCE value of 10.78% (Fig. 6), V_{oc} of 0.96 V, a J_{sc} of 14.92 mA/cm^2 and a FF of 75.3%. To reveal the structure–property relationship of the aromatic side-chain in substituted IDT-based SMDMs as a function of π-bridge and the post annealing conditions, Liu et al. [53] reported a molecule **24** (Chart 2) which showed a PCE of 8.17%, V_{oc} of 0.904 V, J_{sc} of 13.33 mA/cm^2, and a FF of 67% after SVA.

The fabrication of ternary OSCs have attracted much interest

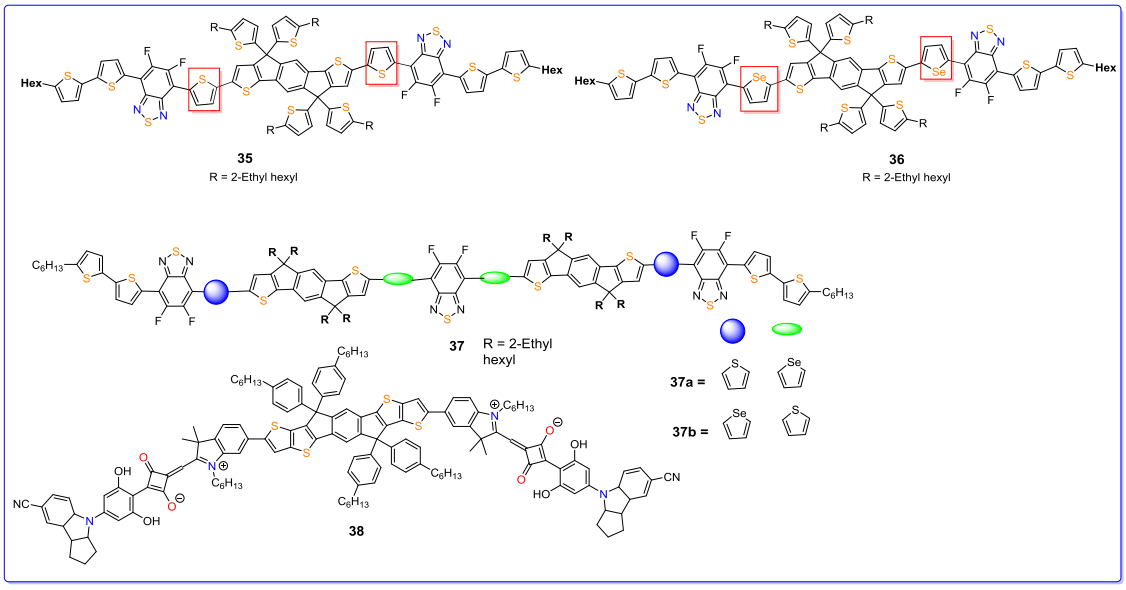

Chart 3. Chemical structures of Indacenodithiophene (IDT)-based SMDMs.

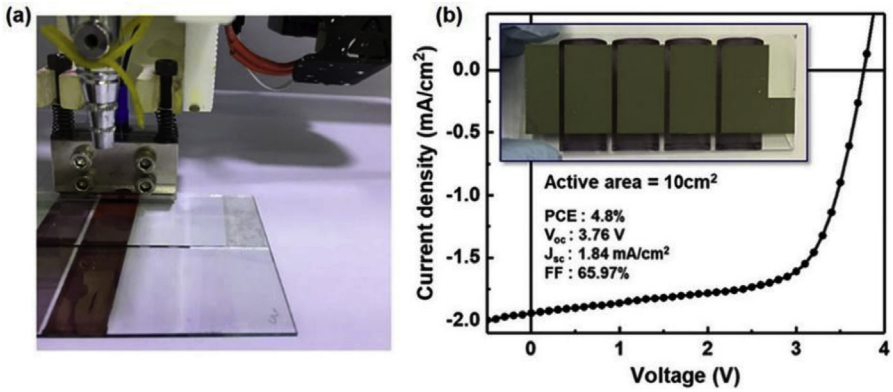

Fig. 4. (a) Photographic image of slot-die-coated large area photovoltaic modules during printing process and (b) corresponding J-V curves cells based on **15**. Reproduced with the permission of Ref. [47].

[54–56] due to the absorption range without the use of complicated tandem cell structures. In this context, Zhang et al. [57] fabricated OSCs of architecture **25**:$PC_{71}BM$ with a PCE of **9.37%**. In order to fabricate a ternary OSC (Fig. 7a), they used small organic molecule DIB-SQ (6 wt %) as the third component in the host **25**:$PC_{71}BM$. The fabricated device shows an incredibly high PCE of 10.3%. This enhancement in PCE is due to increased J_{SC} (15.44 mA/cm^2) and FF (73.8%), which was attributed to the improved photon harvesting of active layer, enhanced energy transfer from **25** to DIB-SQ (Fig. 7b) and molecular packing for efficient exciton dissociation and charge transport.

Similarly, Huang and co-workers [58], fabricated another ternary OSC with the same nematic liquid crystalline SMDM **25** but different polymer donor i.e., **PTB7-Th:$PC_{71}BM$** (Chart 2). The introduction of **25** into the binary system improved the morphology of the blend film, decreased π–π stacking distance, enlarged coherence length, and enhanced domain purity. These modifications led to efficient charge separation, faster charge transport, and lower bimolecular recombination, leading to PCE of 11.40% even with thick active layer (250 nm).

Zhu et al. [59] designed and synthesized a **26** SMD (Chart 2) and the binary device based on it showed a PCE of 5.71% with acceptor $PC_{71}BM$. Furthermore, ternary OSC fabricated by doping 10 wt% of **26** in **PTB7-Th:$PC_{71}BM$**, improved charge-mobility, reduced resistance and better phase separation. This ternary device showed a PCE of 7.77% with a V_{oc} 0.77 V, a J_{SC} 14.52 mA /cm^{2}and a FF of 70.3%. Yang et al. [60] have designed and synthesized a new wide band gap (WBG) SMD **27** (Chart 2) by incorporating a two-dimensional trialkylthienyl-substituted BDT core., The resulting material has band gap (E_g°) of 2.0 eV with a low-lying HOMO level of −5.51 eV. They further constructed a non-fullerene small-molecule organic solar cell (NFSM-OSC) by employing IDIC as an acceptor (Chart 2). The device showed 9.08% PCE with a high V_{oc} (0.98 V). This result demonstrates that the molecular design of a WBG donor to create a well-matched D-A pair with a low band gap (LBG) non-fullerene small-molecule acceptor with a subtle morphological control provides great potential to realize high-performance NFSM-OSCs.

In a similar effort, Qui et al. [61] designed and synthesized two WBG acceptor-donor-acceptor (A-D-A) SMDs bearing electron-withdrawing ester end group with cyano (CN) group **28** and without the cyano group **29** and used acceptor molecule LA-1 (Chart 2). The presence of cyano group on **28** gives the molecule a stronger absorption ($\varepsilon = 8.78 \times 10^4\,M^{-1}\,cm^{-1}$ for **28** and $7.64 \times 10^4\,M^{-1}\,cm^{-1}$ for **29**), lower-lying HOMO energy level and higher charge-mobility compared to the SMD **29**. Film based on **28** and **29** exhibited λ_{max} at 566 and 521 nm which were red-shifted by 66 and 55 nm relative to solution. The device with **28** showed PCE of 10.11% and a high FF (73.55%) compared to molecule **29**, which shows PCE of 5.32%. The results indicate that the cyano substitution in **28** plays an important role in improving the PV performance of the NFSM-OSC. Bin et al. [62] designed and synthesized medium bandgap SMD **30** (Chart 2) with bithienyl-benzodithiophene (BDTT) as central donor unit and fluorobenzotriazole as acceptor unit. They further synthesized a control molecule **31** (Chart 2) without thiophene conjugated side chains on the BDT. The device based on **30** as donor and IDIC as acceptor showed a superior PCE 9.73% compared to device based on **31** with the same configuration. The superiority of **30** based device was attributed to intense absorption, low-lying HOMO energy level, higher hole mobility and ordered bimodal crystallite packing in the blend films. In addition to this a large area (10.0 cm^2) OSC based on **30**:IDIC demonstrated a relatively higher PCE upto **8.52**%. These results clearly attest that fluorobenzotriazole based 2D conjugated organic D-A molecules have a bright future for applications of NFSM-OSC.

Unlike the performance parameters V_{oc} and J_{sc}, optimization of the

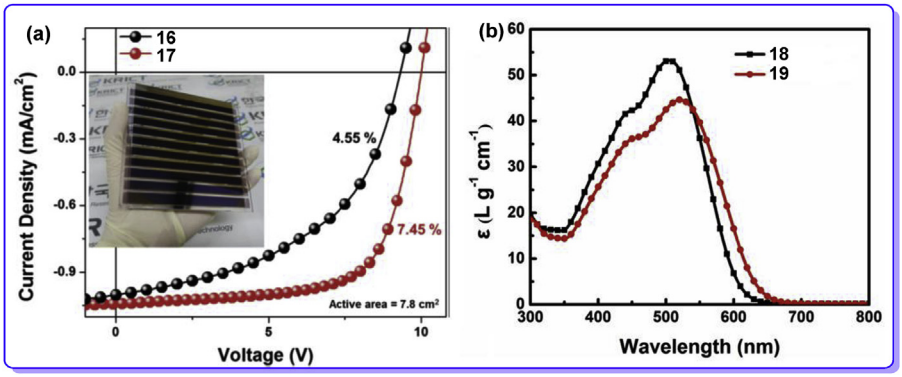

Fig. 5. (a) Characteristic $J - V$ curves for the optimized **16**: $PC_{71}BM$ and **17**:$PC_{71}BM$ large, rigid-module devices (777.5 cm ^{2}) under simulated AM 1.5 G irradiation (b) UV–vis absorption spectra of **18** and **19** in dilute chloroform solutions. Reproduced with the permission of Refs. [48] and [49].

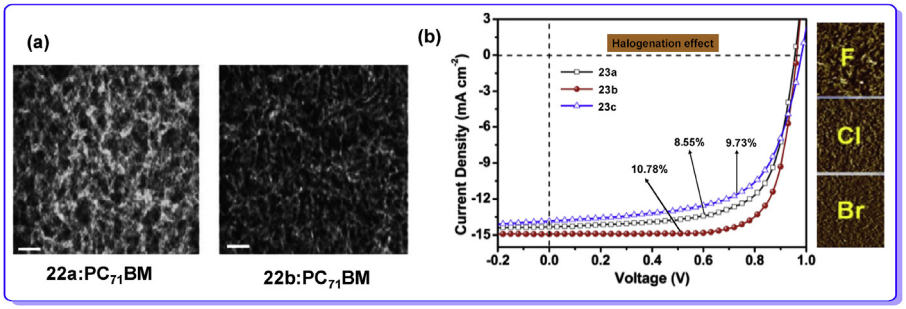

Fig. 6. Transmission electron microscopy (TEM) images of TSA treated **22a**:$PC_{71}BM$ and **22b**:$PC_{71}BM$ thin films; bar is 100 nm and (b) Optimized $J-V$ curves for the SM-OSCs based on **23a-c**. Reproduced with the permission of Refs. [51] and [52].

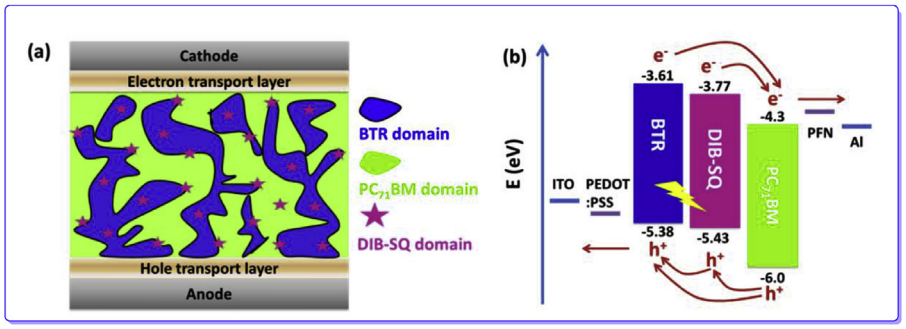

Fig. 7. (a) Schematic diagram of ternary active layer; (b) Energy levels of used materials (arrows represent charge carrier transport direction and lightning bolt represents energy transfer from **25** to DIB-SQ). Reproduced with the permission of Ref. [57].

FF is not so clearly understood [29] to envision high PV performance from the OPV. In order to optimize the FF, Aldrich et al. [63] designed and synthesized a series of small molecules by incorporating the chalcogen (sulphur, oxygen and selenium) into the side chain **32** (Chart 2). It was noted that SMD with higher atomic number (Z) chalcogen shows an enhanced FF value. They found significantly high FF ~8%, which increased on moving from O through S to Se across the series of SMDs. This significant enhancement in the FF was due to the combination of more ordered morphology and decreased charge recombination in blend films for the high-Z chalcogen SMDs. Similarly Wang et al. [64] synthesized SMD **33** (Chart 2), D2-A-D1-A-D2, where D1 an alkylthienyl substituted BDT unit, A represents a tetrazine (Tz) unit, and D2 is a bithiophene or terthiophene ending donor unit. The results of PV study showed that extension of main chain π-conjugation enhanced device performance (V_{oc} = 1.03 V and FF = 65.3% with PCE = 6.49%), while in the side chain leads to larger absorption coefficients, lower HUMO levels, and more favorable blend morphology.

Wan et al. [65] designed and synthesized two SMDs **34a** and **34b** (Chart 2) with benzo[1,2-b:4,5-b′]dithiophene (BDT) as the central donor unit and electron-deficient naphtho[1,2-*c*:5,6-*c*′]bis[1,2,5]thiadiazole (NT) group. This extended the π-conjugation length of the whole small molecular backbone. The introduction of sulphur atom in the side chains further lowered the HOMO/LUMO levels and resulting in a higher V_{oc} (0.93 V) with a very low E_{loss} (0.57 V) for the device **20**. Based on rational material design and device engineering, the resulting SM-OSCs processed with a halogen-free CS_2 solvent exhibited a high efficiency of **11.53%** with a very small energy loss of 0.57 eV.

3.3. Indacenodithiophene (IDT)-based SMDMs

Indacenodithiophene (IDT) is another intriguing class of fragment known for its strong PV potential. Table 3 summarizes the performance of devices based on IDT. Wang et al. [66] reported two tetrafluorinated new SMDs **35** and **36** (Chart 3), consist of electron-rich central core (IDT) and electron-deficient difluorobenzothiadiazole as acceptor units and donor end-capping groups with different π-bridge (thiophene and selenophene). The π-bridge and central core units in these SMDs played an important role in the formation of the nanoscale separation of the blend films. The presence of the electron-rich selenophene spacer in the SMD **36** has prominent effect on the absorption spectrum and molar extinction coefficient which shows a red shift of 20 nm compared to SMD **35** (554 nm). The device based on selenophene spacer i.e., **36**, showed superior PCE (7.31%) with FF ~70% compared to **35** (PCE 5.73% and FF ~ 58%) after annealing due to the optimized morphology and improved charge transport.

With the similar strategy of using the electron-rich selenium, Wang et al. [67] have designed two mixed sulphur and selenium based small molecules **37a** and **37b** (Chart 3), with the selenium and sulphur atoms in different positions. Interestingly, the BHJ-OSC device based on molecule **37b** showed a PCE of 9.3%, which is the highest efficiency based on donor end-capped oligomers. These results clearly demonstrate that a sequence of π-bridge and annealing treatments play important roles for improving ordered and crystalline morphology and enhanced PCE, and therefore provide useful strategy toward highly efficient SMD for BHJ-OSCs.

Despite the fact that SM-OSCs have received considerable attention, a key factor which limits the performance of these small molecules is their large energy loss (E_{loss} 0.6 and 1.0 eV) compared to perovskite and inorganic SCs (E_{loss} < 0.5 eV). In this aspect, Yang et al. [68] designed a new A-D-A type dimeric squarine small donor molecule **38** (Chart 3). The solution of the molecule showed strong absorption which stretches to the NIR region (600–750 nm) with a maximum molar extinction coefficient of $2.84 \times 10^5\ M^{-1}\ cm^{-1}$ at 705 nm due to effective delocalization of the π-electron between their constituent units. The BHJ device fabricated by this low band-gap materials (E_g° = 1.49 eV) exhibited high V_{oc} (0.93 V), high PCE (7.05%) and low E_{loss} (0.56 eV). The result suggests that the A–D–A-structured dimeric molecular strategy can be used as an effective way to obtain low E_{loss} and high V_{oc}, thereby achieving improved performance.

Table 3
Summary of frontier energy levels, device structure and performance parameters of the Indacenodithiophene (IDT)-based SMDMs.

Entry	HOMO/LUMO (eV)	Device architecture	V_{OC} (V)	J_{sc} (mA/cm^2)	FF (%)	PCE (%)	Ref.
35	−5.43/−3.65	ITO/PEDOT:PSS/**35**:$PC_{71}BM$/PFN/Al	0.85	11.17	58.0	5.45	[66]
36	−5.41/−3.67	ITO/PEDOT:PSS/**36**:$PC_{71}BM$/PFN/Al	0.82	12.62	69.0	7.16	[66]
37a	−5.24/−3.19	ITO/PEDOT:PSS/**37a**:**$PC_{71}BM$**/PFN/Al	0.85	11.23	67.0	6.44	[67]
37b	−5.28/−3.22	ITO/PEDOT:PSS/**37b**:**$PC_{71}BM$**/PFN/Al	0.87	14.30	72.0	9.26	[67]

PEDOT:PSS = poly(3,4-ethylenedioxythiophene):polystyrene sulfonate, PFN = poly(9,9-bis(3′-(N,N-dimethylamino)propyl)fluorene-2,7-diyl)-alt-(9,9-dioctyl-fluorene-2,7-diyl).

4. Conclusion and future outlook

During the last three years, the active materials for OPV have grown enormously in PCE and broke the threshold (10%) for potential commercial viability. The progress in the design of small organic donor molecule has slowed down a bit; nevertheless, it is promising. The challenges of preventing recombination, absorbing more broadly and strongly in the visible to near-infrared part of the solar spectrum, and optimizing morphological characteristics to facilitate charge transport still remain. But the steady ongoing progress made towards overcoming these obstacles coupled with the easy tunability and versatility of small organic molecule based donor materials point to a bright future for their continued success as solar energy materials.

Acknowledgements

MSK thanks His Majesty's Trust Fund for Strategic Research (Grant No. SR/SQU/SCI/CHEM/16/02) for funding. MSK also acknowledges The Research Council, Oman (Grant ORG/EI/SQU/13/015) and HM's Trust Fund, Oman for post-doctoral fellowships to RI and AH, respectively.

References

[1] P.-L. Ong, I. Levitsky, Organic/IV, III-V semiconductor hybrid solar cells, Energy 3 (2010) 313.
[2] D.M. Powell, M.T. Winkler, H.J. Choi, C.B. Simmons, D.B. Needleman, T. Buonassisi, Crystalline silicon photovoltaics: a cost analysis framework for determining technology pathways to reach baseload electricity costs, Energy Environ. Sci. 5 (2012) 5874–5883.
[3] C.A. Wolden, J. Kurtin, J.B. Baxter, I. Repins, S.E. Shaheen, J.T. Torvik, A.A. Rockett, V.M. Fthenakis, E.S. Aydil, Photovoltaic manufacturing: present status, future prospects, and research needs, J. Vac. Sci. Technol. Vac. Surf. Films 29 (2011) 030801.
[4] Y. Okamoto, W. Brenner, Organic Semiconductors, Reinhold Pub. Corp, 1964.
[5] M.A. Green, K. Emery, Y. Hishikawa, W. Warta, E.D. Dunlop, D.H. Levi, A.W.Y. Ho-Baillie, Solar cell efficiency tables (version 49), Prog. Photovoltaics Res. Appl. 25 (2017) 3–13.
[6] M.C. Scharber, D. Mühlbacher, M. Koppe, P. Denk, C. Waldauf, A.J. Heeger, C.J. Brabec, Design rules for donors in bulk-heterojunction solar cells—towards 10 % energy-conversion efficiency, Adv. Mater. 18 (2006) 789–794.
[7] C.W. Tang, A.C. Albrecht, Photovoltaic effects of metal–chlorophyll-a–metal sandwich cells, J. Chem. Phys. 62 (1975) 2139–2149.
[8] C.W. Tang, Two-layer organic photovoltaic cell, Appl. Phys. Lett. 48 (1986) 183–185.
[9] L. Yang, S. Zhang, C. He, J. Zhang, H. Yao, Y. Yang, Y. Zhang, W. Zhao, J. Hou, New wide band gap donor for efficient fullerene-free all-small-molecule organic solar cells, J. Am. Chem. Soc. 139 (2017) 1958–1966.
[10] D. Deng, Y. Zhang, J. Zhang, Z. Wang, L. Zhu, J. Fang, B. Xia, Z. Wang, K. Lu, W. Ma, Z. Wei, Fluorination-enabled Optimal Morphology Leads to over 11% Efficiency for Inverted Small-molecule Organic Solar Cells vol. 7, (2016), p. 13740.
[11] W. Zhao, S. Li, H. Yao, S. Zhang, Y. Zhang, B. Yang, J. Hou, Molecular optimization enables over 13% efficiency in organic solar cells, J. Am. Chem. Soc. 139 (2017) 7148–7151.
[12] A. Salleo, R.J. Kline, D.M. DeLongchamp, M.L. Chabinyc, Microstructural characterization and charge transport in thin films of conjugated polymers, Adv. Mater. 22 (2010) 3812–3838.
[13] T.D. Anthopoulos, B. Singh, N. Marjanovic, N.S. Sariciftci, A.M. Ramil, H. Sitter, M. Colle, D.M. de Leeuw, High performance n-channel organic field-effect transistors and ring oscillators based on C-60 fullerene films, Appl. Phys. Lett. 89 (2006) 213504.
[14] D.J. Gundlach, K.P. Pernstich, G. Wilckens, M. Gruter, S. Haas, B. Batlogg, High mobility n-channel organic thin-film transistors and complementary inverters, J. Appl. Phys. 98 (2005) 064502.
[15] J. Roncali, Molecular bulk heterojunctions: an emerging approach to organic solar cells, Acc. Chem. Res. 42 (2009) 1719–1730.
[16] T. Ameri, G. Dennler, C. Lungenschmied, C.J. Brabec, Organic tandem solar cells: a review, Energy Environ. Sci. 2 (2009) 347–363.
[17] K.A. Mazzio, C.K. Luscombe, The future of organic photovoltaics, Chem. Soc. Rev. 44 (2015) 78–90.
[18] M.S. Khan, M.K. Al-Suti, J. Maharaja, A. Haque, R. Al-Balushi, P.R. Raithby, Conjugated poly-ynes and poly(metalla-ynes) incorporating thiophene-based spacers for solar cell (SC) applications, J. Organomet. Chem. 812 (2016) 13–33.
[19] O. Ostroverkhova, Organic optoelectronic materials: mechanisms and applications, Chem. Rev. 116 (2016) 13279–13412.
[20] H. Huang, J. Huang, Organic and Hybrid Solar Cells, Springer International Publishing, 2014.
[21] V. Shrotriya, G. Li, Y. Yao, T. Moriarty, K. Emery, Y. Yang, Accurate measurement and characterization of organic solar cells, Adv. Funct. Mater. 16 (2006) 2016–2023.
[22] H. Jun, M. Careem, A. Arof, Quantum dot-sensitized solar cells—perspective and recent developments: a review of Cd chalcogenide quantum dots as sensitizers, Renew. Sustain. Energy Rev. 22 (2013) 148–167.
[23] K.C. Vijay, L. Cabau, E. Koukaras, G. Sharma, E. Palomares, Synthesis, optical and electrochemical properties of the A-π-D-π-A porphyrin and its application as an electron donor in efficient solution processed bulk heterojunction solar cells, Nanoscale 7 (2014) 179–189.
[24] F. Monestier, J.-J. Simon, P. Torchio, L. Escoubas, F. Flory, S. Bailly, R. de Bettignies, S. Guillerez, C. Defranoux, Modeling the short-circuit current density of polymer solar cells based on P3HT: PCBM blend, Sol. Energy Mater. Sol. Cells 91 (2007) 405–410.
[25] G.F. Burkhard, E.T. Hoke, M.D. McGehee, Accounting for interference, scattering, and electrode absorption to make accurate internal quantum efficiency measurements in organic and other thin solar cells, Adv. Mater. 22 (2010) 3293–3297.
[26] A. Gadisa, M. Svensson, M.R. Andersson, O. Inganäs, Correlation between oxidation potential and open-circuit voltage of composite solar cells based on blends of polythiophenes/fullerene derivative, Appl. Phys. Lett. 84 (2004) 1609–1611.
[27] K. Vandewal, K. Tvingstedt, A. Gadisa, O. Inganas, J.V. Manca, On the origin of the open-circuit voltage of polymer-fullerene solar cells, Nat. Mater. 8 (2009) 904–909.
[28] L.J.A. Koster, V.D. Mihailetchi, R. Ramaker, P.W.M. Blom, Light intensity dependence of open-circuit voltage of polymer:fullerene solar cells, Appl. Phys. Lett. 86 (2005) 123509.
[29] D. Bartesaghi, I.d.C. Pérez, J. Kniepert, S. Roland, M. Turbiez, D. Neher, L.J.A. Koster, Competition between Recombination and Extraction of Free Charges Determines the Fill Factor of Organic Solar Cells vol. 6, (2015), p. 7083.
[30] A. Mishra, P. Baeuerle, Small molecule organic semiconductors on the move: promises for future solar energy technology, Angew. Chem. Int. Ed. 51 (2012) 2020–2067.
[31] Y. Lin, Y. Li, X. Zhan, Small molecule semiconductors for high-efficiency organic photovoltaics, Chem. Soc. Rev. 41 (2012) 4245–4272.
[32] Z. Li, G. He, X. Wan, Y. Liu, J. Zhou, G. Long, Y. Zuo, M. Zhang, Y. Chen, Solution processable rhodanine-based small molecule organic photovoltaic cells with a power conversion efficiency of 6.1%, Adv. Energy Mater. 2 (2012) 74–77.
[33] Z. Wang, Z. Li, J. Liu, J. Mei, K. Li, Y. Li, Q. Peng, Solution-processable small molecules for high-performance organic solar cells with rigidly fluorinated 2,2′-bithiophene central cores, ACS Appl. Mater. Interfaces 8 (2016) 11639–11648.
[34] L. Liang, X.-Q. Chen, X. Xiang, J. Ling, W. Shao, Z. Lu, J. Li, W. Wang, W.-S. Li, Searching proper oligothiophene segment as centre donor moiety for isoindigo-based small molecular photovoltaic materials, Org. Electron. 42 (2017) 93–101.
[35] H. Zhang, Y. Liu, Y. Sun, M. Li, B. Kan, X. Ke, Q. Zhang, X. Wan, Y. Chen, Developing high-performance small molecule organic solar cells via a large planar structure and an electron-withdrawing central unit, Chem. Commun. 53 (2017) 451–454.
[36] J. Hong, J.Y. Choi, T.K. An, M.J. Sung, Y. Kim, Y.-H. Kim, S.-K. Kwon, C.E. Park, A novel small molecule based on dithienophosphole oxide for bulk heterojunction solar cells without pre- or post-treatments, Dyes Pigments 142 (2017) 516–523.
[37] K.H. Park, Y.J. Kim, G.B. Lee, T.K. An, C.E. Park, S.-K. Kwon, Y.-H. Kim, Recently advanced polymer materials containing dithieno[3,2-b:2′,3′-d]phosphole oxide for efficient charge transfer in high-performance solar cells, Adv. Funct. Mater. 25 (2015) 3991–3997.
[38] Y. Ren, T. Baumgartner, Combining form with function - the dawn of phosphole-based functional materials, Dalton Trans. 41 (2012) 7792–7800.
[39] C.-T. Chen, F.-Y. Tsai, C.-Y. Chiang, C.-P. Chen, Spiro-shaped cis-stilbene/fluorene hybrid template for the fabrication of small-molecule bulk heterojunction solar cells, J. Phys. Chem. C 121 (2017) 15943–15948.

[40] W. Wang, P. Shen, X. Dong, C. Weng, G. Wang, H. Bin, J. Zhang, Z.-G. Zhang, Y. Li, Development of spiro[cyclopenta[1,2-b:5,4-b′]dithiophene-4,9′-fluorene]-based a-π-d-π-a small molecules with different acceptor units for efficient organic solar cells, ACS Appl. Mater. Interfaces 9 (2017) 4614–4625.
[41] J. Zhou, X. Wan, Y. Liu, Y. Zuo, Z. Li, G. He, G. Long, W. Ni, C. Li, X. Su, Y. Chen, Small molecules based on benzo[1,2-b:4,5-b′]dithiophene unit for high-performance solution-processed organic solar cells, J. Am. Chem. Soc. 134 (2012) 16345–16351.
[42] W. Ni, M. Li, X. Wan, H. Feng, B. Kan, Y. Zuo, Y. Chen, A high-performance photovoltaic small molecule developed by modifying the chemical structure and optimizing the morphology of the active layer, RSC Adv. 4 (2014) 31977–31980.
[43] B. Kan, Q. Zhang, M. Li, X. Wan, W. Ni, G. Long, Y. Wang, X. Yang, H. Feng, Y. Chen, Solution-processed organic solar cells based on dialkylthiol-substituted benzodithiophene unit with efficiency near 10%, J. Am. Chem. Soc. 136 (2014) 15529–15532.
[44] C. Cui, X. Guo, J. Min, B. Guo, X. Cheng, M. Zhang, C.J. Brabec, Y. Li, High-performance organic solar cells based on a small molecule with alkylthio-thienyl-conjugated side chains without extra treatments, Adv. Mater. 27 (2015) 7469–7475.
[45] M. Li, F. Liu, X. Wan, W. Ni, B. Kan, H. Feng, Q. Zhang, X. Yang, Y. Wang, Y. Zhang, Y. Shen, T.P. Russell, Y. Chen, Subtle balance between length scale of phase separation and domain purification in small-molecule bulk-heterojunction blends under solvent vapor treatment, Adv. Mater. 27 (2015) 6296–6302.
[46] K. Sun, Z. Xiao, S. Lu, W. Zajaczkowski, W. Pisula, E. Hanssen, J.M. White, R.M. Williamson, J. Subbiah, J. Ouyang, A.B. Holmes, W.W. Wong, D.J. Jones, A molecular nematic liquid crystalline material for high-performance organic photovoltaics, Nat. Commun. 6 (2015) 6013.
[47] Y.-J. Heo, Y.-S. Jung, K. Hwang, J.-E. Kim, J.-S. Yeo, S. Lee, Y.-j. Jeon, D. Lee, D.-Y. Kim, Small molecule organic photovoltaic modules fabricated via halogen-free solvent system with roll-to-roll compatible scalable printing method, ACS Appl. Mater. Interfaces 9 (2017) 39519–39525.
[48] S. Badgujar, G.-Y. Lee, T. Park, C.E. Song, S. Park, S. Oh, W.S. Shin, S.-J. Moon, J.-C. Lee, S.K. Lee, High-performance small molecule via tailoring intermolecular interactions and its application in large-area organic photovoltaic modules, Adv. Energy Mater. 6 (2016) 1600228-n/a.
[49] Y.-Q. Guo, Y. Wang, L.-C. Song, F. Liu, X. Wan, H. Zhang, Y. Chen, Small molecules with asymmetric 4-Alkyl-8-alkoxybenzo[1,2-b:4,5-b′]dithiophene as the central unit for high-performance solar cells with high fill factors, Chem. Mater. 29 (2017) 3694–3703.
[50] N.D. Eastham, A.S. Dudnik, B. Harutyunyan, T.J. Aldrich, M.J. Leonardi, E.F. Manley, M.R. Butler, T. Harschneck, M.A. Ratner, L.X. Chen, M.J. Bedzyk, F.S. Melkonyan, A. Facchetti, R.P.H. Chang, T.J. Marks, Enhanced light absorption in fluorinated ternary small-molecule photovoltaics, ACS Energy Lett. 2 (2017) 1690–1697.
[51] M.R. Busireddy, N.R. Chereddy, B. Shanigaram, B. Kotamarthi, S. Biswas, G.D. Sharma, J.R. Vaidya, Dithieno[3,2-b:2[prime or minute],3[prime or minute]-d]pyrrole-benzo[c][1,2,5]thiadiazole conjugate small molecule donors: effect of fluorine content on their photovoltaic properties, Phys. Chem. Chem. Phys. 19 (2017) 20513–20522.
[52] Z. Ji, X. Xu, G. Zhang, Y. Li, Q. Peng, Synergistic effect of halogenation on molecular energy level and photovoltaic performance modulations of highly efficient small molecular materials, Nanomater. Energy 40 (2017) 214–223.
[53] W. Liu, Z. Zhou, T. Vergote, S. Xu, X. Zhu, A thieno[3,4-b]thiophene-based small-molecule donor with a [small pi]-extended dithienobenzodithiophene core for efficient solution-processed organic solar cells, Mater. Chem. Front. 1 (2017) 2349–2355.
[54] Q. An, F. Zhang, J. Zhang, W. Tang, Z. Deng, B. Hu, Versatile ternary organic solar cells: a critical review, Energy Environ. Sci. 9 (2016) 281–322.
[55] L. Lu, M.A. Kelly, W. You, L. Yu, Status and prospects for ternary organic photovoltaics, Nat. Photon. 9 (2015) 491.
[56] T. Ameri, P. Khoram, J. Min, C.J. Brabec, Organic ternary solar cells: a review, Adv. Mater. 25 (2013) 4245–4266.
[57] M. Zhang, J. Wang, F. Zhang, Y. Mi, Q. An, W. Wang, X. Ma, J. Zhang, X. Liu, Ternary small molecule solar cells exhibiting power conversion efficiency of 10.3%, Nanomater. Energy 39 (2017) 571–581.
[58] G. Zhang, K. Zhang, Q. Yin, X.-F. Jiang, Z. Wang, J. Xin, W. Ma, H. Yan, F. Huang, Y. Cao, High-performance ternary organic solar cell enabled by a thick active layer containing a liquid crystalline small molecule donor, J. Am. Chem. Soc. 139 (2017) 2387–2395.
[59] K. Zhu, D. Tang, K. Zhang, Z. Wang, L. Ding, Y. Liu, L. Yuan, J. Fan, B. Song, Y. Zhou, Y. Li, A two-dimension-conjugated small molecule for efficient ternary organic solar cells, Org. Electron. 48 (2017) 179–187.
[60] L. Yang, S. Zhang, C. He, J. Zhang, H. Yao, Y. Yang, Y. Zhang, W. Zhao, J. Hou, New wide band gap donor for efficient fullerene-free all-small-molecule organic solar cells, J. Am. Chem. Soc. 139 (2017) 1958–1966.
[61] B. Qiu, L. Xue, Y. Yang, H. Bin, Y. Zhang, C. Zhang, M. Xiao, K. Park, W. Morrison, Z.-G. Zhang, Y. Li, All-small-molecule nonfullerene organic solar cells with high fill factor and high efficiency over 10%, Chem. Mater. 29 (2017) 7543–7553.
[62] H. Bin, Y. Yang, Z.-G. Zhang, L. Ye, M. Ghasemi, S. Chen, Y. Zhang, C. Zhang, C. Sun, L. Xue, C. Yang, H. Ade, Y. Li, 9.73% efficiency nonfullerene all organic small molecule solar cells with absorption-complementary donor and acceptor, J. Am. Chem. Soc. 139 (2017) 5085–5094.
[63] T.J. Aldrich, M.J. Leonardi, A.S. Dudnik, N.D. Eastham, B. Harutyunyan, T.J. Fauvell, E.F. Manley, N. Zhou, M.R. Butler, T. Harschneck, M.A. Ratner, L.X. Chen, M.J. Bedzyk, R.P.H. Chang, F.S. Melkonyan, A. Facchetti, T.J. Marks, Enhanced fill factor through chalcogen side-chain manipulation in small-molecule photovoltaics, ACS Energy Lett. (2017) 2415–2421.
[64] C. Wang, C. Li, S. Wen, P. Ma, G. Wang, C. Wang, H. Li, L. Shen, W. Guo, S. Ruan, Enhanced photovoltaic performance of tetrazine-based small molecules with conjugated side chains, ACS Sustain. Chem. Eng. 5 (2017) 8684–8692.
[65] J. Wan, X. Xu, G. Zhang, Y. Li, K. Feng, Q. Peng, Highly efficient halogen-free solvent processed small-molecule organic solar cells enabled by material design and device engineering, Energy Environ. Sci. 10 (2017) 1739–1745.
[66] J.-L. Wang, K.-K. Liu, S. Liu, F. Liu, H.-B. Wu, Y. Cao, T.P. Russell, Applying thienyl side chains and different π-bridge to aromatic side-chain substituted indacenodithiophene-based small molecule donors for high-performance organic solar cells, ACS Appl. Mater. Interfaces 9 (2017) 19998–20009.
[67] J.-L. Wang, K.-K. Liu, S. Liu, F. Xiao, Z.-F. Chang, Y.-Q. Zheng, J.-H. Dou, R.-B. Zhang, H.-B. Wu, J. Pei, Y. Cao, Donor end-capped hexafluorinated oligomers for organic solar cells with 9.3% efficiency by engineering the position of π-bridge and sequence of two-step annealing, Chem. Mater. 29 (2017) 1036–1046.
[68] D. Yang, H. Sasabe, T. Sano, J. Kido, Low-band-gap small molecule for efficient organic solar cells with a low energy loss below 0.6 eV and a high open-circuit voltage of over 0.9 V, ACS Energy Lett. 2 (2017) 2021–2025.